

Effect of Electron-Phonon Interactions on Orbital Fluctuations in Iron-Based Superconductors

Yusuke Nomura,¹ Kazuma Nakamura,² and Ryotaro Arita^{1,3}

¹*Department of Applied Physics, University of Tokyo, 7-3-1 Hongo, Bunkyo-ku, Tokyo 113-8656, Japan*

²*Quantum Physics Section, Kyushu Institute of Technology, 1-1 Sensui-cho, Tobata, Kitakyushu, Fukuoka 804-8550, Japan*

³*JST-PRESTO, Kawaguchi, Saitama 332-0012, Japan*

(Received 8 May 2013; published 15 January 2014)

To investigate the possibility of whether electron-phonon coupling can enhance orbital fluctuations in iron-based superconductors, we develop an *ab initio* method to construct the effective low-energy models including the phonon-related terms. With the derived effective electron-phonon interactions and phonon frequencies, we estimate the static part ($\omega = 0$) of the phonon-mediated effective on site intra- or interorbital electron-electron attractions as ~ -0.4 eV and exchange or pair-hopping terms as ~ -0.02 eV. We analyze the model with the derived interactions together with the Coulomb repulsions within the random phase approximation. We find that the enhancement of the orbital fluctuations due to the electron-phonon interactions is small, and that the spin fluctuations enhanced by the Coulomb repulsions dominate. It leads to the superconducting state with the sign reversal in the gap functions (s_{\pm} wave).

DOI: 10.1103/PhysRevLett.112.027002

PACS numbers: 74.70.Xa, 63.20.dk, 74.20.Rp, 74.25.Kc

Introduction.—The mechanism of superconductivity in iron-based superconductors has attracted much attention owing to its high critical temperature (T_c) [1]. The pairing symmetry of the Cooper pair is a central issue and in active debate. There are two strong candidates. One is the spin-fluctuation-mediated s_{\pm} pairing with a sign reversal in the gap functions [2–11], which is consistent with the phase sensitive experiments [12,13]. The other is the orbital-fluctuation-mediated s_{++} pairing without sign changes [14–16], which seems to be compatible with the robustness of the superconductivity against impurity doping [17,18]. As for the orbital fluctuations, it has recently been proposed that not only the Coulomb interactions but also the electron-phonon (*e-ph*) couplings can play a role [14,15]. To examine the scenario quantitatively and conclude the controversy on the pairing symmetry, it is highly required to derive, from first principles, the effective model both with the electronic and the phononic part and analyze it. While the *ab initio* derivations of the electronic model have widely been done [19–24], that for the phonon-related part has not been performed due to the lack of methodology.

In this Letter, we present an *ab initio* effective low-energy model including phonon terms for the iron-based superconductor, LaFeAsO. The effective *e-ph* interactions and phonon frequencies in the model are estimated using the density-functional perturbation theory (DFPT) [25] with a constraint that screening processes in the Fe-3*d* bands are excluded. From the derived parameters, we estimated the phonon-mediated on site electron-electron (*e-e*) attractions. The resulting values for the static part are ~ -0.4 eV for the intra- and interorbital terms and ~ -0.02 eV for the exchange and pair-hopping ones. The magnitude of the obtained exchange interaction is

considerably smaller than the one which gives the s_{++} -wave solution ~ -0.4 eV [14].

We analyzed the model including electronic repulsions as well as the derived phonon-mediated interactions within the random phase approximation (RPA). Because of the small phonon-mediated on site exchange and pair-hopping interactions, the enhancement of the orbital fluctuations is small, and the spin fluctuations enhanced by Coulomb repulsions are dominant and mediate the s_{\pm} -wave pairing.

Method.—Here, we describe the *ab initio* downfolding method to evaluate the *e-ph* couplings and the phonon frequencies in the effective model. The model consists of the phonons and the electronic degrees of freedom belonging to the subspace near the Fermi level, which we call target subspace (*t* subspace). In the case of LaFeAsO, we choose the Hilbert space spanned by the Fe-3*d* bands as the *t* subspace. In this low-energy model, the degrees of freedom residing far from the Fermi level are eliminated, which give the renormalization for the effective parameters [26,27]. We consider the renormalization effects by calculating partially screened (renormalized) *e-ph* couplings and phonon frequencies with excluding the *t*-subspace contribution, which is to be accounted when the model is solved [28–30]. This exclusion is achieved by imposing a constraint to the DFPT calculation. Below, we describe the basic idea and practical treatments.

The frequency for phonon mode ν with momentum \mathbf{q} is determined by the secular equation $\sum_{\kappa'\alpha'} [C_{\kappa\kappa'}^{\alpha\alpha'}(\mathbf{q}) - M_{\kappa}\omega_{\mathbf{q}\nu}^2\delta_{\kappa\kappa'}\delta_{\alpha\alpha'}]e_{\kappa}^{\alpha'}(\mathbf{q}\nu) = 0$ with M_{κ} and α being the mass of atom κ and the Cartesian components, respectively. The interatomic force constants $C_{\kappa\kappa'}^{\alpha\alpha'}(\mathbf{q})$ are given by $C_{\kappa\kappa'}^{\alpha\alpha'}(\mathbf{q}) = \text{bare } C_{\kappa\kappa'}^{\alpha\alpha'}(\mathbf{q}) + \text{ren. } C_{\kappa\kappa'}^{\alpha\alpha'}(\mathbf{q})$, where

$$\text{ren} C_{\kappa\kappa'}^{\alpha\alpha'}(\mathbf{q}) = \frac{1}{N} \int \left[\frac{\partial n(\mathbf{r})}{\partial u_{\kappa}^{\alpha}(\mathbf{q})} \right]^* \frac{\partial V_{\text{ion}}(\mathbf{r})}{\partial u_{\kappa'}^{\alpha'}(\mathbf{q})} d\mathbf{r}, \quad (1)$$

with N , $n(\mathbf{r})$, $u(\mathbf{q})$, and $V_{\text{ion}}(\mathbf{r})$ being the number of unit cells in the crystal, electron density, ionic displacement, and ionic potential, respectively. Here, $\text{ren} C_{\kappa\kappa'}^{\alpha\alpha'}(\mathbf{q})$ gives the renormalization of the phonon frequencies via the linear e -ph coupling, and $\text{bare} C_{\kappa\kappa'}^{\alpha\alpha'}(\mathbf{q})$ gives the bare phonon frequencies [31]. The e -ph couplings are evaluated as $g_{n'n}^{\nu}(\mathbf{k}, \mathbf{q}) = \sum_{\kappa\alpha} e_{\kappa}^{\alpha}(\mathbf{q}\nu) d_{n'n}^{\kappa\alpha}(\mathbf{k}, \mathbf{q}) / \sqrt{2M_{\kappa}\omega_{\mathbf{q}\nu}}$, where $d_{n'n}^{\kappa\alpha}(\mathbf{k}, \mathbf{q}) = \langle \psi_{n'\mathbf{k}+\mathbf{q}} | \partial V_{\text{SCF}}(\mathbf{r}) / \partial u_{\kappa}^{\alpha}(\mathbf{q}) | \psi_{n\mathbf{k}} \rangle$ is a coupling between the Bloch states $\psi_{n\mathbf{k}}$ with momentum \mathbf{k} and band n and $\psi_{n'\mathbf{k}+\mathbf{q}}$. The derivative of the self-consistent field potential $\partial V_{\text{SCF}}(\mathbf{r}) / \partial u_{\kappa}^{\alpha}(\mathbf{q})$ is written as

$$\frac{\partial V_{\text{SCF}}(\mathbf{r})}{\partial u_{\kappa}^{\alpha}(\mathbf{q})} = \frac{\partial V_{\text{ion}}(\mathbf{r})}{\partial u_{\kappa}^{\alpha}(\mathbf{q})} + \int \left[\frac{e^2}{|\mathbf{r}-\mathbf{r}'|} + \frac{dV_{\text{xc}}(\mathbf{r})}{dn} \delta(\mathbf{r}-\mathbf{r}') \right] \times \frac{\partial n(\mathbf{r}')}{\partial u_{\kappa}^{\alpha}(\mathbf{q})} d\mathbf{r}', \quad (2)$$

with $V_{\text{xc}}(\mathbf{r})$ being the exchange-correlation potential. In the rhs of this formula, the first term denotes the bare potential and the second one denotes the screening potential. The electron density response $\partial n(\mathbf{r}) / \partial u_{\kappa}^{\alpha}(\mathbf{q})$ in Eqs. (1) and (2) gives the renormalization of the phonon frequencies and the screening for the e -ph couplings. This response is explicitly written as

$$\frac{\partial n(\mathbf{r})}{\partial u_{\kappa}^{\alpha}(\mathbf{q})} = 2 \sum_{nm\mathbf{k}} \frac{f_{n\mathbf{k}} - f_{m\mathbf{k}+\mathbf{q}}}{\varepsilon_{n\mathbf{k}} - \varepsilon_{m\mathbf{k}+\mathbf{q}}} \psi_{n\mathbf{k}}^*(\mathbf{r}) \psi_{m\mathbf{k}+\mathbf{q}}(\mathbf{r}) d_{mn}^{\kappa\alpha}(\mathbf{k}, \mathbf{q}), \quad (3)$$

where $\varepsilon_{n\mathbf{k}}$ and $f_{n\mathbf{k}}$ are the eigenvalue and its occupancy, respectively.

For the derivation of the effective model, we calculate the density response with excluding the contribution from the case where both $\psi_{m\mathbf{k}+\mathbf{q}}$ and $\psi_{n\mathbf{k}}$ belong to the t subspace. Then, with the resulting density response, we evaluate the partially screened (renormalized) quantities such as $g^{(p)}$ and $\omega^{(p)}$. We call the scheme ‘‘constrained DFPT (cDFPT)’’. Without the constraint, fully screened quantities are calculated, to which we attach the superscript ‘‘ f ’’, instead of ‘‘ p ’’ [33].

Now, we write down the phonon-related terms in the effective model. The effective e -ph interactions are

$$\mathcal{H}_{e\text{-ph}} = \frac{1}{\sqrt{N_{\mathbf{k}}}} \sum_{\mathbf{q}\nu} \sum_{\mathbf{k}i\sigma} g_{ij}^{(p)\nu}(\mathbf{k}, \mathbf{q}) c_{i\mathbf{k}+\mathbf{q}}^{\sigma\dagger} c_{j\mathbf{k}}^{\sigma} (b_{\mathbf{q}\nu} + b_{-\mathbf{q}\nu}^{\dagger}), \quad (4)$$

where $b_{\mathbf{q}\nu}$ ($b_{\mathbf{q}\nu}^{\dagger}$) is the annihilation (creation) operator of the phonon with the wave vector \mathbf{q} and the branch ν . $c_{i\mathbf{k}}^{\sigma}$ ($c_{i\mathbf{k}}^{\sigma\dagger}$) annihilates (creates) the i -th Wannier orbital’s electron with the wave vector \mathbf{k} and the spin σ . $N_{\mathbf{k}}$ is the number of \mathbf{k} points. The phonon one-body part is given as

$$\mathcal{H}_{\text{ph}} = \sum_{\mathbf{q}\nu} \omega_{\mathbf{q}\nu}^{(p)} b_{\mathbf{q}\nu}^{\dagger} b_{\mathbf{q}\nu}. \quad (5)$$

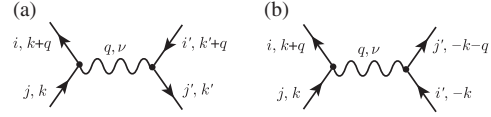


FIG. 1. Feynman diagrams for phonon-mediated effective (a) e - e [Eq. (6)] and (b) pairing [Eq. (7)] interactions. Solid lines with arrows are electron propagators, wavy lines are phonon Green’s functions, and dots represent e -ph couplings.

The momentum-space-averaged phonon-mediated effective e - e interaction $V_{ij,i'j'}^{(p)}$ [Fig. 1(a)] is given by

$$V_{ij,i'j'}^{(p)}(\omega_l) = \frac{1}{N_{\mathbf{q}}} \sum_{\mathbf{q}\nu} \left(\frac{1}{N_{\mathbf{k}}} \sum_{\mathbf{k}} g_{ij}^{(p)\nu}(\mathbf{k}, \mathbf{q}) \right) D_{\mathbf{q}\nu}^{(p)}(\omega_l) \times \left\{ \frac{1}{N_{\mathbf{k}}} \sum_{\mathbf{k}'} [g_{i'j'}^{(p)\nu}(\mathbf{k}', \mathbf{q})]^* \right\}, \quad (6)$$

where $\omega_l = 2\pi lT$ is the boson Matsubara frequency and $D_{\mathbf{q}\nu}^{(p)}(\omega_l) = -2\omega_{\mathbf{q}\nu}^{(p)} / (\omega_l^2 + \omega_{\mathbf{q}\nu}^{(p)2})$. Note that $V_{ij,i'j'}^{(p)}$ corresponds to the on site quantity because of the momentum-space averaging. This $V_{ij,i'j'}^{(p)}$ is distinguished from the momentum-space-averaged phonon-mediated effective pairing interaction $V'_{ij,i'j'}^{(p)}$ [Fig. 1(b)] as

$$V'_{ij,i'j'}^{(p)}(\omega_l) = \frac{1}{N_{\mathbf{q}} N_{\mathbf{k}}} \sum_{\mathbf{q}\nu} \sum_{\mathbf{k}} g_{ij}^{(p)\nu}(\mathbf{k}, \mathbf{q}) D_{\mathbf{q}\nu}^{(p)}(\omega_l) [g_{i'j'}^{(p)\nu}(\mathbf{k}, \mathbf{q})]^*. \quad (7)$$

Results.—We performed density-functional calculations with QUANTUM ESPRESSO package [34]. The generalized-gradient approximation with the Perdew-Burke-Ernzerhof parameterization [35] and the Troullier-Martins norm-conserving pseudopotentials [36] in the Kleinman-Bylander representation [37] are adopted. The cutoff energy for the wave functions is set to 95 Ry, and we employ $8 \times 8 \times 6$ \mathbf{k} points. The phonon frequencies and the e -ph interactions are calculated using the DFPT [25] with and without the constraint, where $4 \times 4 \times 3$ \mathbf{q} mesh and a Gaussian smearing of 0.02 Ry are employed. The maximally localized Wannier function [38] is used as the basis of the model. The lattice parameter and the internal coordinates are fully optimized and we get $a = 4.0344$ Å, $c = 8.9005$ Å, $z_{\text{La}} = 0.14233$, and $z_{\text{As}} = 0.63330$. These values are in good agreement with those of Refs. [39,40].

We show in Fig. 2(a) our calculated band structure (solid curves) of LaFeAsO with the optimized structure and compare with the Wannier-interpolated band (dotted ones) for the Fe-3 d orbitals. Hereafter, $d_{3Z^2-R^2}$, d_{XZ} , d_{YZ} , $d_{X^2-Y^2}$, and d_{XY} orbitals are represented as 1, 2, 3, 4, and 5, respectively, where the X and Y axes are parallel to the nearest Fe-As bonds and the Z axis is perpendicular to the FeAs layer. The screening and self-energy effects within the energy range from the bottom of the Fe-3 d bands up to 2.32 eV are excluded to derive $g^{(p)}$ and $\omega^{(p)}$.

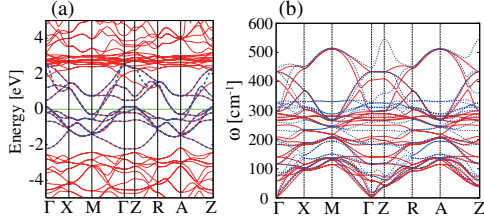


FIG. 2 (color online). (a) Band structure of LaFeAsO for the optimized structure (red solid curves). Blue dotted curves denote the Wannier-interpolated band dispersion. (b) Fully (red solid curves) and partially (blue dotted curves) renormalized phonon dispersion of LaFeAsO.

Figure 2(b) displays our calculated phonon dispersions with (dotted curves) and without (solid ones) the constraint on the t -subspace screening. We see a discernible difference in the frequencies for the phonon modes which couple to the t -subspace electrons. However, the difference is not large, at most $\sim 20\%$.

Table I lists our calculated static on site phonon-mediated interactions. The upper left-side two 5×5 matrices are the e - e interaction $V_{ij,i'j'}^{(p)}(0)$ in Eq. (6). The intra- and interorbital terms $V_{ii,jj}^{(p)}(0)$ are ~ -0.4 eV, while the exchange and pair-hopping terms $V_{ij,ij}^{(p)}(0) = V_{ij,ji}^{(p)}(0)$ are rather small as ~ -0.02 eV. Compared to the on site Coulomb repulsion $U \sim 2$ eV [23], $V_{ii,ii}^{(p)}(0) \sim -0.4$ eV are not negligible. However, it should be noted here that, while $U(\omega_l)$ is almost constant up to the typical plasmon frequency (~ 25 eV in the iron-based superconductors [41]), the attractions $V_{ij,i'j'}^{(p)}(\omega_l)$ quickly decay as ω_l increases and vanish around $\omega_l \sim \omega_D$ with ω_D being the Debye frequency.

TABLE I. Our calculated static phonon-mediated effective electron-electron interaction $V_{ij,i'j'}(\omega_l=0)$ and pairing interaction $V'_{ij,i'j'}(\omega_l=0)$. Note that the values are represented with the negative sign. The upper (lower) panel shows the partially (fully) screened interactions. $V_{ij,i'j'}$ is symmetric with respect to $i \leftrightarrow j$, $i' \leftrightarrow j'$, and $(ij) \leftrightarrow (i'j')$. $V'_{ij,i'j'}$ is symmetric with respect to $(i'j') \leftrightarrow (jj')$ and $(ij) \leftrightarrow (i'j')$. Units are given in eV.

$-V_{ii,jj}^{(p)}$					$-V_{ij,ij}^{(p)} (= -V_{ij,ji}^{(p)}) \times 10$					$-V'_{ii,jj}^{(p)}$					$-V'_{ij,ji}^{(p)}$					$-V'_{ij,ij}^{(p)} \times 10$						
1	2	3	4	5	2	3	4	5	1	2	3	4	5	2	3	4	5	2	3	4	5	2	3	4	5	
1	0.47	0.44	0.44	0.38	0.44	0.23	0.23	0.21	0.03	0.57	0.49	0.49	0.33	0.44	0.09	0.09	0.22	0.12	0.001	0.001	0.41	0.61	0.001	0.001	0.41	0.61
2	...	0.43	0.41	0.36	0.42	...	0.06	0.20	0.23	...	0.52	0.48	0.27	0.46	...	0.10	0.16	0.14	...	-0.21	-0.21	0.28	...	-0.21	-0.21	0.28
3	0.43	0.36	0.42	0.20	0.23	0.52	0.27	0.46	0.16	0.14	-0.21	0.28	-0.21	0.28
4	0.32	0.35	0.03	0.54	0.23	0.08	-0.03	-0.03
5	0.43	0.69

$-V_{ii,jj}^{(f)} \times 10$					$-V_{ij,ij}^{(f)} (= -V_{ij,ji}^{(f)}) \times 10$					$-V'_{ii,jj}^{(f)} \times 10$					$-V'_{ij,ji}^{(f)}$					$-V'_{ij,ij}^{(f)} \times 10$						
1	2	3	4	5	2	3	4	5	1	2	3	4	5	2	3	4	5	2	3	4	5	2	3	4	5	
1	0.27	0.28	0.28	0.24	0.21	0.25	0.25	0.24	0.01	1.80	0.97	0.97	-0.46	0.32	0.13	0.13	0.31	0.17	-0.11	-0.11	0.86	0.98	-0.11	-0.11	0.86	0.98
2	...	0.37	0.24	0.27	0.21	...	0.03	0.14	0.18	...	1.60	1.05	-0.89	1.07	...	0.15	0.22	0.18	...	-0.30	-0.57	0.14	...	-0.30	-0.57	0.14
3	0.37	0.27	0.21	0.14	0.18	1.60	-0.89	1.07	0.22	0.18	-0.57	0.14	-0.57	0.14
4	0.39	0.11	0.04	3.48	-1.87	0.12	-0.02	-0.02
5	0.28	4.33

The three matrices in the upper right side of Table I are the effective pairing interactions $V'_{ij,i'j'}(0)$ in Eq. (7). Because of the off site pairing interactions, the pair-hopping terms $V'_{ij,ji}(0)$ are substantially larger in magnitude than the on site quantities $V'_{ii,ii}(0)$.

The lower part of Table I describes fully screened ones $V_{ij,i'j'}^{(f)}(0)$ and $V'_{ij,i'j'}(0)$. The intra- and interorbital terms are efficiently screened from the t -subspace electrons, while others are not. We note that the quantity $\sum_{ij} V_{ij,ji}^{(f)} N_i(0) N_j(0) / N(0)$ with $N_i(0)$ [$N(0)$] being the partial [total] density of states at the Fermi level is ~ 0.18 , which gives a reasonable estimate to the total e -ph coupling constant $\lambda \sim 0.2$ in this system [39].

Effect on pairing symmetry.—Here, we analyze a five-band model including the electronic repulsions and phonon-mediated interactions within the RPA. The calculation detail follows Refs. [14,15]. The spin and charge susceptibilities are given by $\hat{\chi}^{s(c)}(q) = \hat{\chi}^0(q) [1 - \hat{\Gamma}^{s(c)} \hat{\chi}^0(q)]^{-1}$, where $\hat{\chi}^0(q)$ is the irreducible susceptibility and $\Gamma_{ij,i'j'}^s = U, U', J, \text{ and } J'$ for $i=j=i'=j'$, $i=i' \neq j=j'$, $i=j \neq i'=j'$, $i=j' \neq i'=j$, respectively, [14]. U (U') is the intra- (inter)orbital Coulomb repulsion, J is the Hund's coupling, and J' is the pair hopping. The matrix $\hat{\Gamma}^c$ is given by $\hat{\Gamma}^c = -\hat{C} - 2\hat{V}^{(p)}(\omega_l)$, where $C_{ij,i'j'} = U, -U' + 2J, 2U' - J, \text{ and } J'$ for $i=j=i'=j'$, $i=i' \neq j=j'$, $i=j \neq i'=j'$, $i=j' \neq i'=j$, respectively, [14].

With these susceptibilities, we solve the linearized gap equation

$$\lambda_E \Delta_{i'j'}(k) = \frac{T}{N} \sum_{k',j_i} W_{ij_1,j_4i'}(k-k') G_{j_1j_2}^0(k') \times \Delta_{j_2j_3}(k') G_{j_4j_3}^0(-k'), \quad (8)$$

where $\Delta_{i'i'}(k)$ [$G_{i'i'}^0(k)$] is the gap (noninteracting Green's) function in the orbital representation and $W_{ij,i'j'}(q)$ is the pairing interaction kernel. For the singlet pairing, $\hat{W}(q) = -\frac{3}{2}\hat{\Gamma}^s\hat{\chi}^s(q)\hat{\Gamma}^s + \frac{1}{2}\hat{\Gamma}^c\hat{\chi}^c(q)\hat{\Gamma}^c - \frac{1}{2}(\hat{\Gamma}^s - \hat{\Gamma}^{vc})$ with $\hat{\Gamma}^{vc} = -\hat{C} - 2\hat{V}^{(p)}(\omega_l)$ [42]. The eigenvalue λ_E grows as the temperature decreases, reaching unity at the superconducting transition temperature.

We adopt two dimensional model and 64×64 \mathbf{k} -point meshes and 2048 Matsubara frequencies are taken. The temperature and the filling are set to $T = 0.02$ eV and $n = 6.1$, respectively. We discuss the structure of the diagonal elements of the gap-function matrices in the band representation at the lowest Matsubara frequency and we denote them as $\varphi_m(\mathbf{k})$ with m being the band index. When the Coulomb interactions are large, the RPA treatment is known to be unstable [3]. So, we scale the original *ab initio* electronic interactions U , U' , J , and J' [45] by 1/2 with keeping the phonon-mediated interactions $V_{ij,i'j'}^{(p)}$ and $V_{ij,i'j'}^{(p)}$ at the original values in Table I.

Our calculated gap functions $\varphi_2(\mathbf{k})$, $\varphi_3(\mathbf{k})$, and $\varphi_4(\mathbf{k})$ are shown in Figs. 3(a), 3(b), and 3(c), respectively. We see the sign change in the gap functions on the Fermi surfaces (FS's); i.e., the s_{\pm} -wave state is realized. In our parameter setting, the phonon-mediated interactions are considerably over-emphasized to the scaled electronic repulsions; nevertheless, we get the s_{\pm} -wave solution. Thus, the s_{++} -wave pairing based on the orbital fluctuations due to the e -ph interactions would not be realized in the *ab initio* parameter range [46].

To clarify why the s_{\pm} -wave state is stable even if we introduce the e -ph interactions, we analyze simpler models. We use the following Coulomb parameters: $U = 0.8$ eV, $U' = 0.69U$, and $J = J' = 0.16U$. For the phonon-mediated interaction matrix \hat{V} [47], we consider two parameter sets. One is the same as that of Ref. [14]; the exchange terms $V_{ij,ij}$ are set to be equal to the intraorbital ones $V_{ii,ii}$ such as $V_{24,24} = V_{34,34} = V_{22,22} = V_{33,33} = -V_{22,33} = V(\omega_l)$, where $V(\omega_l) = V(0)\omega_D^2/(\omega_l^2 + \omega_D^2)$ with $V(0) = -0.385$ eV and $\omega_D = 0.02$ eV [48]. Note that $V_{ij,i'j'}$ has the symmetry on the index interchange as $i \leftrightarrow j$, $i' \leftrightarrow j'$, and

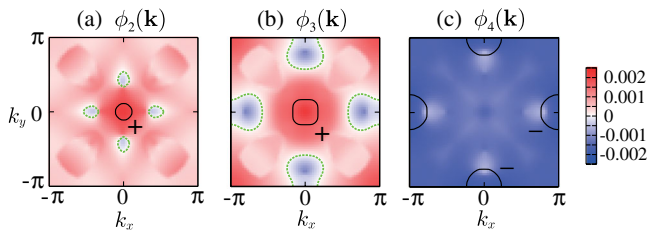


FIG. 3 (color online). RPA results for the gap functions (a) φ_2 , (b) φ_3 , and (c) φ_4 . We used $T = 0.02$ eV and $n = 6.1$. As for the interaction parameters, we scaled the *ab initio* Coulomb interactions in Ref. [23] by 1/2, while we used the original values in Table I for the phonon-mediated e - e interactions. The black-solid (green-dotted) curves represent the FS's (nodes of the gap functions), together with the sign of gap functions on each FS's.

$(ij) \leftrightarrow (i'j')$. The other parameter set is based on the present *ab initio* results; the exchange terms are appreciably weakened from the intra- and interorbital ones; $V_{24,24} = V_{34,34} = V(\omega_l)/20$ and $V_{22,22} = V_{33,33} = V_{22,33} = V(\omega_l)$. With the former parameter set, we see an enhancement of the orbital fluctuations and get the s_{++} -wave state, while, in the latter case, the spin fluctuations enhanced by the Coulomb repulsions develop and bring about the s_{\pm} -wave pairing. In the analysis for the former case, we checked that the sign change of $V_{22,33}$ has no qualitative effect on the pairing symmetry. Therefore, it is deduced that the magnitudes of $V_{24,24}$ and $V_{34,34}$ are crucial in determining s_{++} - or s_{\pm} -wave states.

When the exchange and pair-hopping terms $V_{24,24} = V_{24,42} = V_{34,34} = V_{34,43}$ are large in magnitude, the scattering channels $W_{24,42}$ and $W_{34,43}$, which connect Δ_{44} and Δ_{22} , and Δ_{44} and Δ_{33} , respectively, are enhanced through the charge sector and both channels have the positive value [14]. These attractive pairing channels lead to the same sign in Δ_{22} , Δ_{33} , and Δ_{44} . Since the FS's consist of these three (2-4) orbitals, the s_{++} -wave state is realized. On the other hand, when $V_{24,24}$ and $V_{34,34}$ are small as with the *ab initio* results, the scattering channels enhanced by the spin part become dominant and the s_{\pm} -wave state is realized. Thus, the e -ph interactions with the *ab initio* energy scale alone cannot drive the orbital-fluctuation-mediated s_{++} -wave pairing [49].

Conclusion.—We have developed an *ab initio* downfolding method for e -ph coupled systems and applied it to the derivation of the effective model of LaFeAsO. With the derived effective e -ph interactions $g^{(p)}$ and phonon frequencies $\omega^{(p)}$, we have estimated the phonon-mediated effective on site e - e interactions as $V_{ii,ii}^{(p)}(0) \sim V_{ii,jj}^{(p)}(0) \sim -0.4$ eV and $V_{ij,ij}^{(p)}(0) = V_{ij,ji}^{(p)}(0) \sim -0.02$ eV. We have analyzed the derived five band model consisting of Fe-3d bands using the RPA. The s_{++} -wave pairing is not realized with the *ab initio* e -ph interaction with the tiny exchange and pair-hopping terms, and the s_{\pm} -wave state mediated by spin-fluctuations is robustly realized.

While our study is concentrated on LaFeAsO, it would be interesting to perform a comprehensive cDFPT study for the other iron-based superconductors including those with different topology of Fermi surfaces [52–55], and investigate the material dependence. Furthermore, our developed cDFPT also enables the quantitative study of other superconductors and different areas of research related to phonons, such as multiferroics, thermoelectric materials, dielectrics, and polaron problems. These applications are interesting and important future issues.

We would like to thank Hiroshi Kontani, Seiichiro Onari, Hiroaki Ikeda, Ryosuke Akashi, and Hideyuki Miyahara for fruitful discussions. This work was supported by Funding Program for World-Leading Innovative R&D on Science and Technology (FIRST program) on “Quantum Science on Strong Correlation” JST-PRESTO, Grants-in-Aid for Scientific Research (Grants No. 22740215,

No. 22104010, No. 23110708, No. 23340095, No. 23510120, No. 25800200) and the Next Generation Super Computing Project and Nanoscience Program from MEXT, Japan. Y.N. is supported by the Grant-in-Aid for JSPS Fellows (Grant No. 12J08652).

-
- [1] G. R. Stewart, *Rev. Mod. Phys.* **83**, 1589 (2011).
- [2] I. I. Mazin, D. J. Singh, M. D. Johannes, and M. H. Du, *Phys. Rev. Lett.* **101**, 057003 (2008).
- [3] K. Kuroki, S. Onari, R. Arita, H. Usui, Y. Tanaka, H. Kontani, and H. Aoki, *Phys. Rev. Lett.* **101**, 087004 (2008).
- [4] H. Ikeda, *J. Phys. Soc. Jpn.* **77**, 123707 (2008).
- [5] A. V. Chubukov, D. V. Efremov, and I. Eremin, *Phys. Rev. B* **78**, 134512 (2008).
- [6] T. Nomura, *J. Phys. Soc. Jpn.* **78**, 034716 (2009).
- [7] F. Wang, H. Zhai, Y. Ran, A. Vishwanath, and D.-H. Lee, *Phys. Rev. Lett.* **102**, 047005 (2009).
- [8] Z.-J. Yao, J.-X. Li, and Z. D. Wang, *New J. Phys.* **11**, 025009 (2009).
- [9] R. Arita and H. Ikeda, *J. Phys. Soc. Jpn.* **78**, 113707 (2009).
- [10] A. F. Kemper, T. A. Maier, S. Graser, H.-P. Cheng, P. J. Hirschfeld, and D. J. Scalapino, *New J. Phys.* **12**, 073030 (2010).
- [11] R. M. Fernandes and J. Schmalian, *Phys. Rev. B* **82**, 014521 (2010).
- [12] T. Hanaguri, S. Niitaka, K. Kuroki, and H. Takagi, *Science* **328**, 474 (2010).
- [13] C.-T. Chen, C. C. Tsuei, M. B. Ketchen, Z.-A. Ren, and Z. X. Zhao, *Nat. Phys.* **6**, 260 (2010).
- [14] H. Kontani and S. Onari, *Phys. Rev. Lett.* **104**, 157001 (2010).
- [15] T. Saito, S. Onari, and H. Kontani, *Phys. Rev. B* **82**, 144510 (2010).
- [16] Y. Yanagi, Y. Yamakawa, and Y. Ōno, *Phys. Rev. B* **81**, 054518 (2010).
- [17] Y. Kobayashi, A. Kawabata, S.-C. Lee, T. Moyoshi, and M. Sato, *J. Phys. Soc. Jpn.* **78**, 073704 (2009); M. Sato, Y. Kobayashi, S.-C. Lee, H. Takahashi, E. Satomi, and Y. Miura, *ibid.* **79**, 014710 (2010).
- [18] S. Onari and H. Kontani, *Phys. Rev. Lett.* **103**, 177001 (2009).
- [19] K. Nakamura, R. Arita, and M. Imada, *J. Phys. Soc. Jpn.* **77**, 093711 (2008).
- [20] T. Miyake, L. Pourovskii, V. Vildosola, S. Biermann, and A. Georges, *J. Phys. Soc. Jpn. Suppl. C* **77**, 99 (2008).
- [21] T. Miyake, K. Nakamura, R. Arita, and M. Imada, *J. Phys. Soc. Jpn.* **79**, 044705 (2010).
- [22] K. Nakamura, Y. Yoshimoto, Y. Nohara, and M. Imada, *J. Phys. Soc. Jpn.* **79**, 123708 (2010).
- [23] T. Misawa, K. Nakamura, and M. Imada, *Phys. Rev. Lett.* **108**, 177007 (2012).
- [24] M. Hirayama, T. Miyake, and M. Imada, *Phys. Rev. B* **87**, 195144 (2013).
- [25] S. Baroni, S. de Gironcoli, A. Dal Corso, and P. Giannozzi, *Rev. Mod. Phys.* **73**, 515 (2001).
- [26] G. Kotliar, S. Y. Savrasov, K. Haule, V. S. Oudovenko, O. Parcollet, and C. A. Marianetti, *Rev. Mod. Phys.* **78**, 865 (2006).
- [27] M. Imada and T. Miyake, *J. Phys. Soc. Jpn.* **79**, 112001 (2010).
- [28] F. Aryasetiawan, M. Imada, A. Georges, G. Kotliar, S. Biermann, and A. I. Lichtenstein, *Phys. Rev. B* **70**, 195104 (2004).
- [29] J. Bauer, J. E. Han, and O. Gunnarsson, *Phys. Rev. B* **84**, 184531 (2011).
- [30] R. Nourafkan, F. Marsiglio, and G. Kotliar, *Phys. Rev. Lett.* **109**, 017001 (2012).
- [31] See Supplemental Material at <http://link.aps.org/supplemental/10.1103/PhysRevLett.112.027002> for the explicit form of ${}^{\text{bare}}C_{\kappa\kappa'}^{aa'}(\mathbf{q})$ (Ref. [32]).
- [32] See Supplemental Material at <http://link.aps.org/supplemental/10.1103/PhysRevLett.112.027002> for additional information on the cDFPT method.
- [33] The effective parameters for Coulomb interactions are widely derived using the constrained random phase approximation (cRPA) [28]. The comparison between the present cDFPT and the cRPA is given in Supplemental Material in Ref. [32].
- [34] P. Giannozzi *et al.*, *J. Phys. Condens. Matter* **21**, 395502 (2009); <http://www.quantum-espresso.org/>.
- [35] J. P. Perdew, K. Burke, and M. Ernzerhof, *Phys. Rev. Lett.* **77**, 3865 (1996).
- [36] N. Troullier and J. L. Martins, *Phys. Rev. B* **43**, 1993 (1991).
- [37] L. Kleinman and D. M. Bylander, *Phys. Rev. Lett.* **48**, 1425 (1982).
- [38] N. Marzari and D. Vanderbilt, *Phys. Rev. B* **56**, 12 847 (1997); I. Souza, N. Marzari, and D. Vanderbilt, *ibid.* **65**, 035109 (2001).
- [39] L. Boeri, O. V. Dolgov, and A. A. Golubov, *Phys. Rev. Lett.* **101**, 026403 (2008).
- [40] D. J. Singh and M.-H. Du, *Phys. Rev. Lett.* **100**, 237003 (2008).
- [41] P. Werner, M. Casula, T. Miyake, F. Aryasetiawan, A. J. Millis, and S. Biermann, *Nat. Phys.* **8**, 331 (2012).
- [42] In Refs. [43,44], the possibility of the triplet pairing was also pursued.
- [43] A. Aperis, P. Kotetes, G. Varelogiannis, and P. M. Oppeneer, *Phys. Rev. B* **83**, 092505 (2011).
- [44] A. Aperis and G. Varelogiannis, arXiv:1303.2231.
- [45] As for the effective Coulomb interactions, we employ the values in Ref. [23].
- [46] We note that the s_{\pm} -wave state is always realized when we change the scaling parameter for Coulomb interactions from 0.4 to 0.6.
- [47] We use the common phonon-mediated interaction parameters for $\hat{\Gamma}^c$ and $\hat{\Gamma}^{c'}$, i.e., $\hat{\Gamma}^c = \hat{\Gamma}^{c'} = -\hat{C} - 2\hat{V}(\omega_l)$.
- [48] For simplicity, the V terms are introduced only for the 2, 3, and 4 orbitals which compose the FS's, following Ref. [14].
- [49] We find that e -ph interactions do not enhance the orbital fluctuations, but it was recently proposed that the vertex corrections could possibly enhance them [50,51].
- [50] S. Onari and H. Kontani, *Phys. Rev. Lett.* **109**, 137001 (2012).
- [51] H. Miyahara, R. Arita, and H. Ikeda, *Phys. Rev. B* **87**, 045113 (2013).
- [52] J. Guo, S. Jin, G. Wang, S. Wang, K. Zhu, T. Zhou, M. He, and X. Chen, *Phys. Rev. B* **82**, 180520(R) (2010).
- [53] Y. Zhang, L. X. Yang, M. Xu, Z. R. Ye, F. Chen, C. He, H. C. Xu, J. Jiang, B. P. Xie, J. J. Ying, X. F. Wang, X. H. Chen, J. P. Hu, M. Matsunami, S. Kimura, and D. L. Feng, *Nat. Mater.* **10**, 273 (2011).
- [54] T. Qian, X.-P. Wang, W.-C. Jin, P. Zhang, P. Richard, G. Xu, X. Dai, Z. Fang, J.-G. Guo, X.-L. Chen, and H. Ding, *Phys. Rev. Lett.* **106**, 187001 (2011).
- [55] L. Zhao *et al.*, *Phys. Rev. B* **83**, 140508(R) (2011).